

Computational and MR-guided Patient-Specific Laser Induced Thermal Therapy of Cancer

D. Fuentes, J. T. Oden, K. R. Diller, A. Elliott, Y. Feng, J. D. Hazle, A. Shetty, and R. J. Stafford

Abstract This chapter describes the development of a canonical dynamic data driven predictive control system for MR-guided laser induced thermal therapies (MRgLITT) of focal cancerous lesions within soft tissue. The predictive ability of computational models combined with advanced clinical imaging modalities is exploited to plan, predict, control, and optimize the treatment outcome. The system is under continual development and embodies a cyberinfrastructure comprised of Magnetic Resonance Thermal Imaging (MRTI), computer visualization, laser optics, high-speed networks, nonlinear dynamic bioheat transfer models of heterogeneous tissue, adaptive meshing, high-performance parallel computing, cell-damage models, inverse analysis, calibration, model validation, signal processing, optimal control algorithms, and error estimation and control. These diverse technologies and systems are connected across a high-speed computational grid connecting remote sites 150 miles apart and is an excellent example of a Dynamic Data Driven Application System (DDDAS).

Webpage: <http://wiki.ices.utexas.edu/dddas>

A. Elliott, D. Fuentes, J. D. Hazle, A. Shetty, and R. J. Stafford,
The University of Texas M.D. Anderson Cancer Center, Department of Imaging Physics, Houston TX 77030, USA, e-mail: [andrew.elliott, dtfuentes, jhazle, anil.shetty, jstafford]@mdanderson.org

Y. Feng,
Computational Bioengineering and Nanotechnology Lab, The University of Texas at San Antonio, San Antonio, TX 78749, USA, e-mail: yusheng.feng@utsa.edu

K. R. Diller
Department of Biomedical Engineering, The University of Texas at Austin, Austin TX 78712, USA, e-mail: oden@ices.utexas.edu, kdiller@mail.utexas.edu

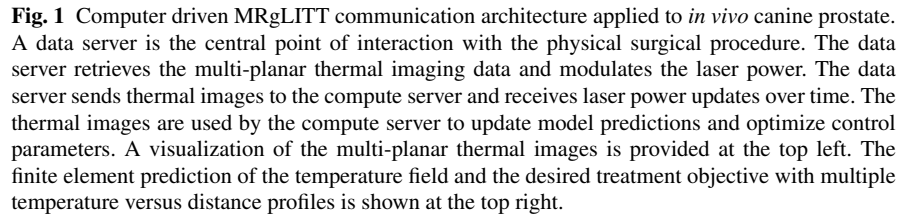
J. T. Oden
Institute for Computational Engineering and Sciences, The University of Texas at Austin, Austin TX 78712, USA, e-mail: oden@ices.utexas.edu

1 Introduction

Laser induced thermal therapy (LITT) is a minimally invasive procedure that replaces the scalpel of conventional surgery and the ionizing radiation of radiosurgery with a $<2\text{mm}$ laser diode applicator minus the typical side effects and morbidity. A specially designed laser fiber is delivered stereotactically or under real-time image-guidance to the site of a tumor and the fundamental idea is that when the laser heats the tumor cells to a certain point, the cells are damaged and die. The heating portion of the procedure takes only a few minutes. MR-guided LITT (MRgLITT) is performed under thermal image monitoring using magnetic resonance thermal imaging (MRTI). The thermal images provide a quantitative treatment time estimate of the lethality of the thermal dose received by the tumor and surrounding healthy tissue. MRgLITT has recently entered into patient use [4]; multiple clinical trials within the United States are currently on-going for an FDA cleared MRgLITT system that utilizes real-time temperature imaging feedback and dosimetry (Visualase®, Visualase, Inc. Houston, TX) and at least one trial for another system (AutoLITT, Monteris Medical, Cleveland, Ohio) is being conducted under an investigational device exemption (IDE).

While real-time temperature monitoring provides invaluable treatment-time feedback that makes the procedure safe and feasible once a laser applicator has been placed, innovations in human assisted high performance computational tools using this feedback are under development to plan, control, predict, and optimize the anticipated biological response to dramatically increase treatment efficacy and reduce associated treatment morbidity and even reduce recurrence of the disease.

DDAS aims at developing a computational system that dynamically interacts with medical imaging technology for the predictive guidance and control of medical procedures. It is a monumentally important development that could enhance many fields of medical science. The unique dynamic closed loop control system presented by the predictive capabilities of computational simulation coupled with real-time multi-planar image guidance as feedback has significant potential to facilitate a reliable minimally invasive treatment modality that delivers an optimized thermal dose prescribed by the physician. The control system developed in this work, Figure 1, employs a cyberinfrastructure [1] of magnetic resonance thermal imaging, computer visualization, laser optics, high-speed networks, nonlinear dynamic bio-heat transfer models of heterogeneous tissue, adaptive meshing, high-performance parallel computing, cell-damage and heat-shock protein models, inverse analysis, calibration, model validation, signal processing, optimal control algorithms, and error estimation and control. A computational grid connects two remote arenas over a high bandwidth network; an imaging and laser treatment arena that manages the thermal data and laser source and a computational arena that uses parallel computing algorithms to generate and solve computational models of bioheat transfer



2 Governing Equations

The equations of bioheat transfer and light transport within laser-irradiated tissue are the fundamental equations used in this work. Elements of continuum mechan-

ics, thermodynamics, anatomy, and physiology are coalesced within the field of bioheat transfer. Biological heat transfer may include conduction, convection, radiation, metabolism, and evaporation. However, the defining characteristic is the biological heat transfer between blood and tissue; blood flow through the complex vasculature networks embedded in tissue may act as a significant heat sink in MRgLITT. The seminal development of the equations of bioheat transfer are attributed to the work of Pennes [20] in 1948. The original Pennes model describes bioheat transfer as the conservation of energy applied to a motionless non-deforming homogeneous mass of human tissue. The model does not allow mass flux across the boundary and assumes a uniform heat source based on the perfusion of blood throughout the tissue. Pennes model has been shown to provide very accurate predictions of biological heat transfer [5, 8, 10, 18, 22, 27]. We employ a nonlinear modification of the Pennes model and allow the thermal conductivity and perfusion model parameters to vary spatially. The initial boundary value model is defined by the following system:

$$\begin{aligned}
\rho c_p \frac{\partial u}{\partial t} - \nabla \cdot (k(\mathbf{x}) \nabla u) + \omega(\mathbf{x}) c_{blood} (u - u_a) &= Q_{laser}(\mathbf{x}, t) \quad \text{in } \Omega \\
Q_{laser}(\mathbf{x}, t) &= 3P(t) \mu_a \mu_{tr} \frac{\exp(-\mu_{eff} \|\mathbf{x} - \mathbf{x}_0\|)}{4\pi \|\mathbf{x} - \mathbf{x}_0\|} \quad \mu_{tr} = \mu_a + \mu_s(1 - g) \\
&\quad \mu_{eff} = \sqrt{3\mu_a \mu_{tr}} \\
-k(u, \mathbf{x}) \nabla u \cdot \mathbf{n} &= h(u - u_\infty) \quad \text{on } \partial\Omega_C \\
-k(u, \mathbf{x}) \nabla u \cdot \mathbf{n} &= \mathcal{G} \quad \text{on } \partial\Omega_N \\
u(\mathbf{x}, 0) &= u^0 \quad \text{in } \Omega
\end{aligned} \tag{1}$$

The measured baseline body temperature is taken as the initial temperature field, u^0 . The density of the continuum, ρ , is homogeneous and the c_{blood} denotes the specific heat. On the Cauchy boundary, $\partial\Omega_C$, u_∞ is the ambient temperature and h is the coefficient of cooling. \mathcal{G} denotes the prescribed heat flux on the Neumann boundary, $\partial\Omega_N$. The classical spherically symmetric isotropic solution to the transport equation of light within a laser-irradiated tissue [26] is used to model optical-thermal response to the laser source, $Q_{laser}(\mathbf{x}, t)$. The anisotropic factor is denoted g and \mathbf{x}_0 denotes the position of laser photon source. $P(t)$ is the laser power as a function of time, μ_a and μ_s are laser coefficients related to laser wavelength and give probability of absorption and scattering of photons, respectively. The perfusion, $\omega(\mathbf{x})$, and thermal conductivity, $k(\mathbf{x})$, are allowed to vary spatially within a local region of interest, $r \approx 1\text{cm}$, around the laser source.

$$k_0(\mathbf{x}) = \begin{cases} k_0, & x \notin \mathcal{B}_r(\mathbf{x}) \\ k_0(\mathbf{x}), & x \in \mathcal{B}_r(\mathbf{x}) \end{cases} \quad \omega_0(\mathbf{x}) = \begin{cases} \omega_0, & x \notin \mathcal{B}_r(\mathbf{x}) \\ \omega_0(\mathbf{x}), & x \in \mathcal{B}_r(\mathbf{x}) \end{cases}$$

The main problems of the control system are the optimal control of the laser source and the calibration of the model parameters with respect to thermal imaging data. The mathematical structure of the calibration and optimal control problems

both fall within the framework of PDE constrained optimization: Find the set of model parameters β^* , that minimizes a given objective function, Q , over a parameter manifold, \mathbb{P} ,

$$\begin{aligned} &\text{Find } \beta^* \in \mathbb{P} \text{ s.t.} \\ &Q(u(\beta^*), \beta^*) = \inf_{\beta \in \mathbb{P}} Q(u(\beta), \beta) \end{aligned}$$

Where β may represent any subset of the model parameters available for optimization, perfusion, thermal conductivity, and laser parameters are highlighted in (1), and the objective function, Q , is of the form of the $L_2(0, T; L_2(\Omega))$ norm of the difference between the predicted temperature field, $u(\mathbf{x}, t)$ and an ideal temperature field $u^{\text{ideal}}(\mathbf{x}, t)$.

$$\begin{aligned} Q(u(\mathbf{x}, t)) &= \frac{1}{2} \|u(\mathbf{x}, t) - u^{\text{ideal}}(\mathbf{x}, t)\|_{L^2(\Delta T; L^2(\Omega))}^2 \\ &= \frac{1}{2} \int_{\Omega} \int_{\Delta T} \left(u(\mathbf{x}, t) - u^{\text{ideal}}(\mathbf{x}, t) \right)^2 dt dx \end{aligned} \quad (2)$$

where $dx = dx_1 dx_2 dx_3$ is a volume element and the time interval of interest is denoted ΔT . u^{ideal} may represent the thermal imaging data for the calibration problem or a desired thermal dose for the optimal control problem. A quasi-Newton optimization solver [3] is used for the PDE constrained optimization problems. The gradient of the objective function (2) is computed using an adjoint method. The derivation of the gradient may be found in [11, 19].

3 Simulation Guided MRgLITT Workflow

An overview of the continually evolving treatment workflow is provided in Table 1. T_1 and T_2 -weighted MRI is the definitive imaging modality for seeing the prostate anatomy and surrounding critical structures. This, in addition to the ability to pro-

Table 1 Treatment Workflow

Pretreatment	Image Acquisition Optimizations Model Predictions	Geometry Extraction Surgeon Interaction
Treatment Setup	Registration Model Predictions	Patient Specific Calibrations Treatment Day Updates
Inter-operative	Real-Time Monitoring Model Updates	Model Control of Delivery
Post Treatment	Prediction Validation	

vide real-time feedback and post-treatment imaging verification of delivery make it an ideal "one-stop-shop" for thermal therapy in the prostate. Several days prior to treatment, the anatomy, the prostate in this case, is scanned using a clinical MR

scanner. This pre-operative, anatomical data is used to create a 3D finite element representation of the geometry of the anatomy, Figure 2. A pipeline of software is used to segment the anatomy, create a faceted surface representation, and generate a high-quality finite element mesh. An experienced user must identify and extract the geometry from the pre-operative images. The faceted surface represents a 3D manifold that is then used to create a volumetric finite element mesh.

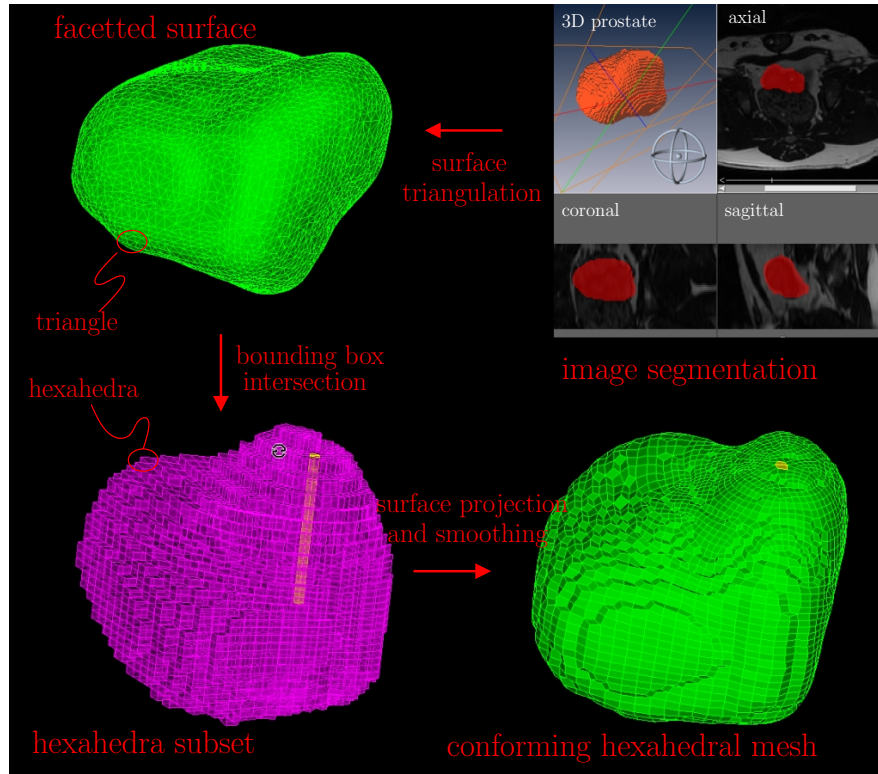


Fig. 2 Anatomical imaging to hexahedral finite element mesh pipeline. The anatomy of interest is labeled for segmentation. The prostate is labeled using a subset of the axial images. The anatomy labels are displayed in the coronal and sagittal planes as well to ensure 3D conformity to the boundary of the anatomy. The labeled voxels corresponding to the prostate are displayed in 3D and a faceted triangulation representing the boundary of the prostate is generated. The intersection of a structured grid and the volume enclosed by the interior of the faceted surface is the base of the hexahedral mesh. The surface of the initial hexahedral mesh is projected toward the boundary of the prostate and the mesh is smoothed.

Given the finite element mesh of the anatomy, initial optimal laser parameters are identified such as the location of the endpoint of the optical fiber and laser power as a function of time. Prior to treatment, mock simulations of the therapy are performed using tabulated bioheat transfer data, Figure 3, and allow the physician to tune the computed optimal delivery. The laser is placed in the prostate using a stereotactic

guide. An actively cooled applicator with 980nm diffusing tip fiber is used to deliver therapy. Laser power is controlled by sending updated powers to the Visualase control system in real-time. The guide, laser, and Visualase control system are all manufactured by BioTex, Inc., Houston, TX. The initial parameters are corrected

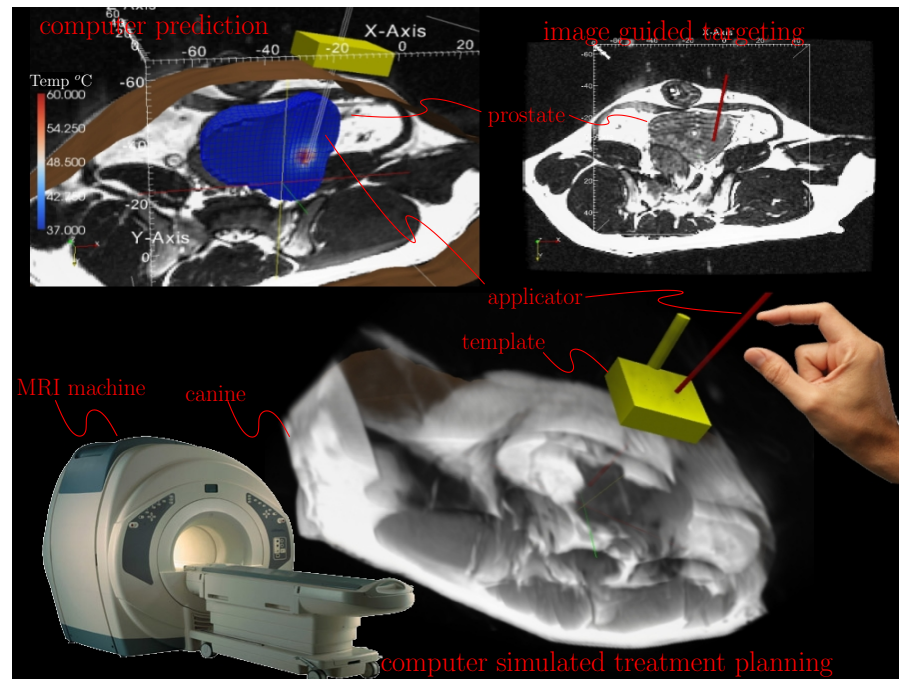


Fig. 3 Computer guided treatment planning. A fiducial marked treatment template is registered to planning images and used to guide the laser applicator. Prior to the procedure, trial simulations of the thermal delivery may be simulated to evaluate the effect of the desired thermal dose to surrounding critical structures. Virtual repositioning of the laser reduces the morbidity associated with physically repositioning the applicator.

during the calibration phase of the process using MRTI generated thermal imaging data. Developed over the past decade, MRTI technology is a modification of existing MRI technology to use temperature sensitive echo planar imaging sequences to acquire larger imaging volumes in the same time with comparable temperature sensitivity and to provide a time varying multi-planar temperature field in the living tissue. The treatment control system is guided by simulations performed at the computational modeling arena. The simulation tools embed thermal imaging data within a Pennes bioheat transfer model constrained optimization framework. Through accurate computer prediction, the bioheat transfer response may be controlled through a collection of imaging based measurements about how the complex physiological system is responding to the surgery and make treatment plan updates based on an

intelligent understanding of the physiological pathways to affect the surgical outcome.

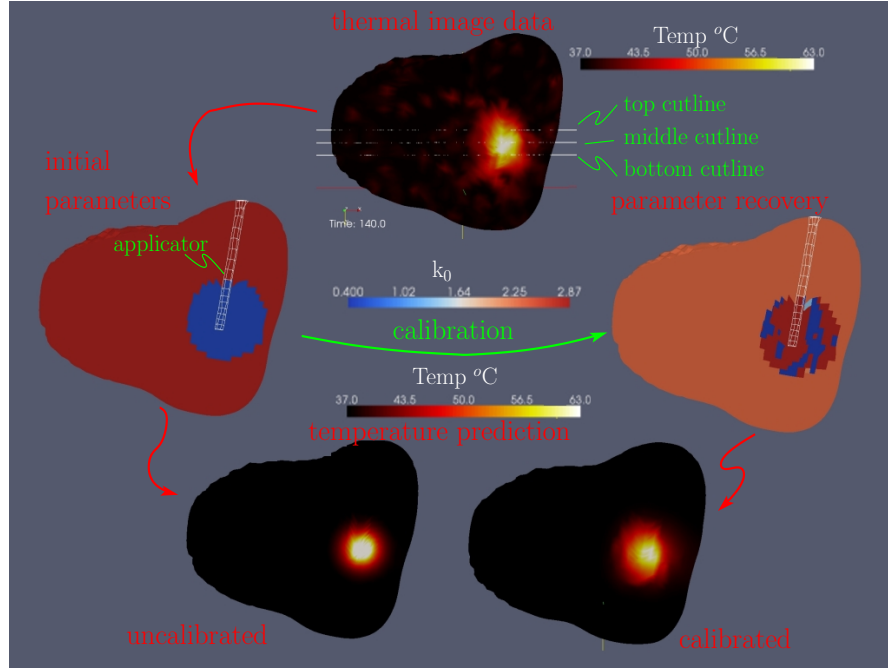


Fig. 4 Model calibration using homogeneous and heterogeneous model parameters. A particular time instance of the thermal imaging data used to drive the model calibrations is shown at the top. The uncalibrated model begins with homogeneous model parameters with different coefficients in the neighborhood of the laser tip, left center. Isotherms of the initial uncalibrated temperature prediction are spherical, as expected from a homogeneous media with a isotropic source term, lower left. As the optimization process recovers spatially varying thermal parameters, center right, isotherms of the model prediction are no longer spherical and are in significantly much better agreement with the thermal imaging data. The difference in the temperature profiles are provided in Figure 5.

4 Results

The DDDAS infrastructure for MRgLITT has been successfully tested *in vivo* canine prostate. The laser induced thermal therapy was performed at M.D. Anderson Cancer Center (MDACC) in Houston, Texas. A non-destructive calibration laser pulse was used to acquire intra-operative real time thermal imaging data of the heating and cooling and calibrate the computational models of bioheat transfer. The bio-heat transfer was controlled to within 5°C of the predetermined treatment plan us-

ing the calibrated models implemented on supercomputers over a distance of 150mi from the treatment site. Real-time remote visualization of the anatomical data, thermal imaging data, FEM prediction, and model parameters of the on-going treatment was provided. The computational requirements imposed an 18 minute treatment time; 3 minutes for delivery of a low power training pulse, 5 minutes of actual therapeutic exposure, and the rest for synchronization and computational overhead. Post operative histology of the canine prostate reveals that the damage region was within the targeted 1.2cm diameter treatment objective. See [11, 13] for further technical details.

In vivo experiments thus far have utilized homogeneous parameter calibration techniques. Heterogeneous model calibration involving thousands of model parameters have been shown to deliver model predictions of unprecedented accuracy [6]. Recent work has demonstrated the feasibility of converging to a solution of a heterogeneous Pennes PDE constrained optimization problem with thousands of model parameters on the scale of minutes [12]. Figure 4 shows the effect of calibrating the tissue models as a heterogeneous linearly conductive media. Allowing the biological thermal properties to vary spatially provides a means to achieve patient specific accuracy in the model prediction. Temperature profiles comparing the difference in the thermal imaging data and model predictions is provided in Figure 5.

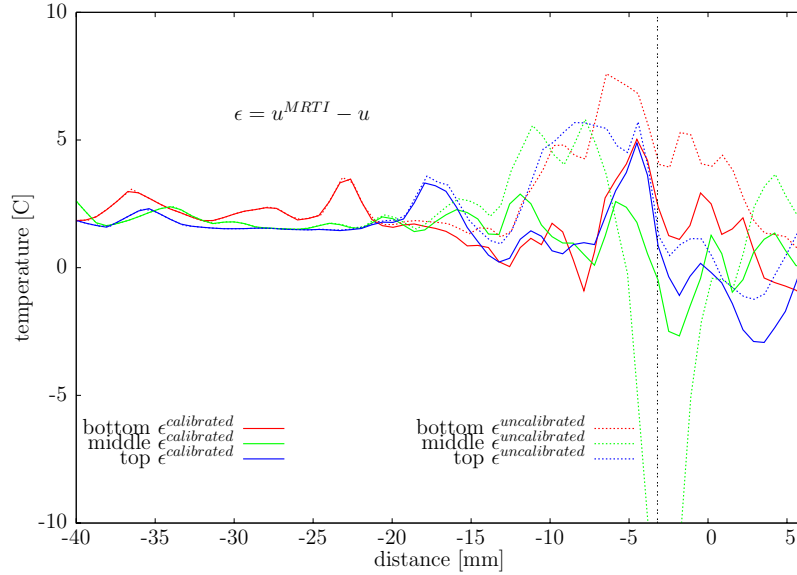


Fig. 5 The difference in the uncalibrated and calibrated temperature profiles predicted by the model. The temperature difference and distance are given in units of degrees Celsius and millimeters, respectively. The position of the top, middle, and bottom profiles are shown in Figure 4. The pointwise difference between the thermal image data and finite element prediction pre- and post-calibration is compared. Similar color graph lines represent corresponding profiles of the calibrated and uncalibrated predictions.

5 Discussion and Future Direction

Results have demonstrated the *feasibility* of designing simulation protocols and methodologies that interact with thermal imaging modalities and provide real-time control of thermal therapies for cancer treatment in a clinical setting. Calibration pulses prior to delivery of the thermal insult can be used to recover heterogeneous biothermal parameters on a patient specific basis. The predictive ability of computational models can be exploited to predict, control, and optimize the treatment. All necessary technologies to realize computer driven MRgLITT within a clinical setting currently exist; magnetic resonance thermal imaging, computer visualization, laser optics, high-speed networks, nonlinear dynamic bioheat transfer models of heterogeneous tissue, adaptive meshing, high-performance parallel computing, cell-damage and heat-shock protein models, inverse analysis, calibration, model validation, signal processing, optimal control algorithms, and error estimation and control. A substantial effort is currently underway to package these technologies into streamlined computational tools similar to those that exist for stereotactic radiosurgery [25].

A suite of hierarchical computational tools for MRgLITT is being developed, Figure 6. Computational tools for prospective 3D treatment planning of MRgLITT forms the software foundation. Tools for prospective treatment planning are a necessary precursor to existing online temperature monitoring technologies. A significant software development effort is needed to streamline protocols and computational visualization interfaces to interact with existing stereotactic technology for treatment time positioning of the thermal applicator. For example, for thermal therapy of prostate, fiducials on the applicator can be registered to planning images and three dimensional visualizations of the anatomy, using either segmented surfaces or volume visualization techniques. The visualizations can provide depth perception for applicator insertion superior to current methodologies that use a series of 2D slices and have led to applicator insertion that can damage surrounding tissues. Further, given the projected applicator position, the thermal dose to the targeted lesion and other critical structures, seminal vesicles, rectum, bladder, may be simulated. Visualization of the percentage of target tissue predicted to have a lethal thermal damage by an Arrhenius model or a two-state model [9] with respect to the desired plan and visualization of surrounding structures, Figure 7, may reveal the necessity of repositioning the laser or early laser power cutoff. The software interface is a crucial component of the system. A user-friendly and portable software infrastructure that will cleanly interact with a variety of commercial imaging modalities will provide a reproducible means of therapy and allow the construction of multi-institutional trials to evaluate this therapy versus conventional modalities.

A substantial amount of work is needed to retrospectively validate and verify the software predictions in phantoms and *in vivo*; the validated models can then be used to answer important therapeutic questions and evaluate the efficacy of the tool for deciding the placement and number of fibers needed to safely and effectively treat a target volume and decrease the need for retreatment and repositioning. Models that recover the patient specific thermal parameters have demonstrated significant

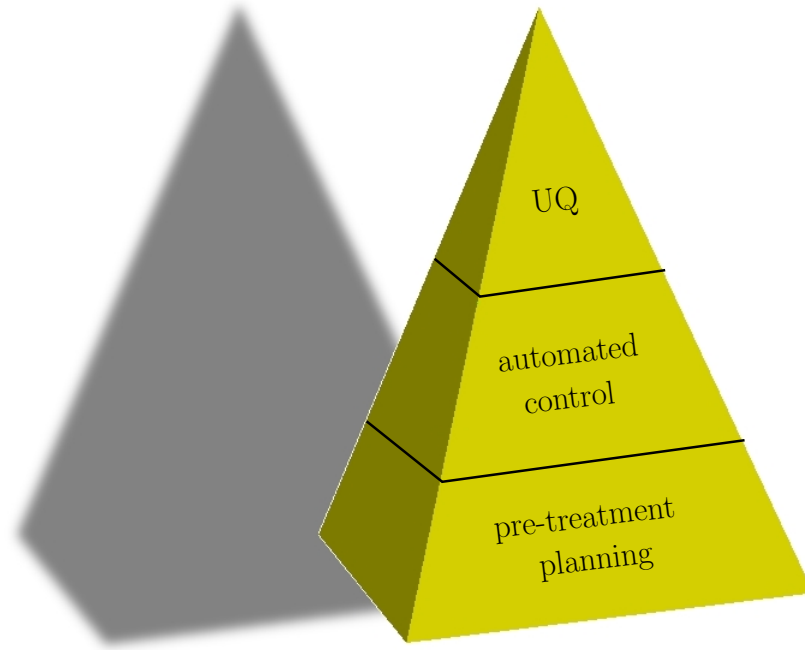


Fig. 6 The translational research involved to realize computer driven MRgLITT within a clinical setting will build upon a hierarchy of methodologies and technologies each increasing in complexity. The customized graphical user interface for visualizing and monitoring thermal image feedback along with computational predictions for pre-treatment planning provides the software foundation. The natural next layer of technology is provided by robust software for automated control of the thermal therapy delivery modality and updating the computational models on a patient specific basis. Software for uncertainty quantification-based decisions and control provides the final step; the degree of confidence in the treatment success, including percentage of target lesion destroyed and an estimated damage to nearby critical structures, will allow surgical oncologists to make informed decisions.

potential in accurately predicting the bioheat transfer and have even been shown to compensate for modeling inaccuracies in the thermal source term. Experiments can be conducted that validate the spatially varying thermal parameters recovered by inverse problems against the actual local physical values. These experiments will require accurate modeling of the laser fluence distribution beyond that provided the isotropic source term presented in this work; either a Monte Carlo source [21] or delta-P[7] model must be used. Physiological factors that locally change the perfusion levels can have a dramatic effect on the upper lesion size limits. Given an expected perfusion rate and the expected upper limit on lesion size, the necessity of using multiple laser applicators may be evaluated. Further, the efficacy in terms of conformal thermal dose and cost of multiple laser applicators can be compared to that obtained using a high laser power from a single applicator. Because of the uses

of laser for therapy delivery, the use of nanoshells may play an important role in the future; an effective distribution of nanoshells that enhances the thermal properties of the media combined with a high laser power may prove to deliver an equivalent lethal conformal thermal dose as multiple applicators.

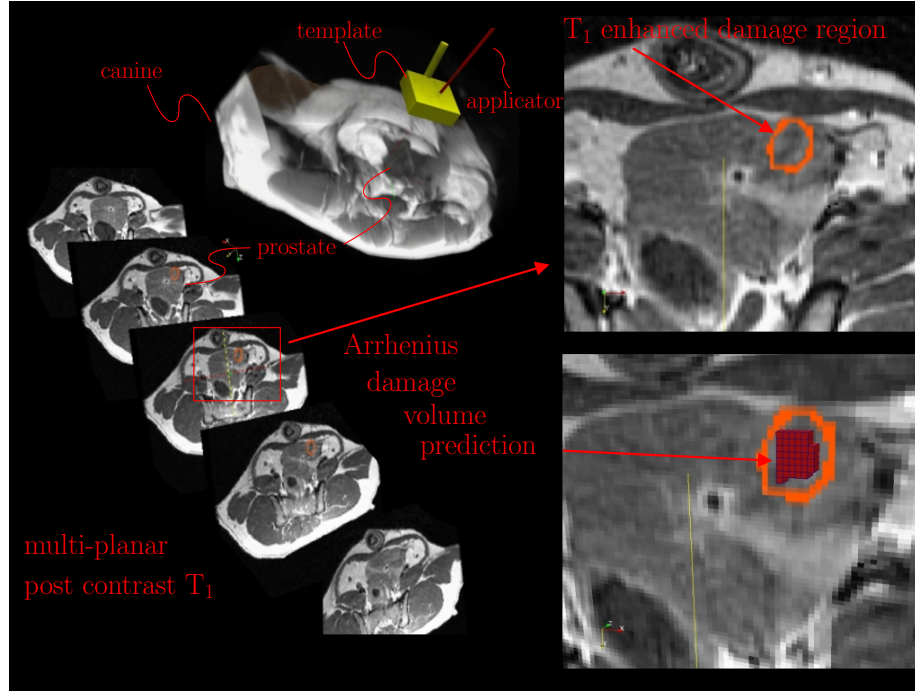


Fig. 7 Post Treatment validation. Post treatment contrast that enhances the T_1 properties of the tissue may be used to validate the damage predicted by an Arrhenius damage model. Using 3D visualization techniques, the damage region may be shown in perspective to the target tissue and surrounding structures.

As the planning software matures and is clinically validated, the computational performance and methodologies will be optimized for computer guided real-time delivery and control. The target of real-time control is to deliver a lethal thermal dose that conforms to the target lesion. Imaging feedback must be used with laser applicator(s) to update the bioheat transfer models to the biological thermal properties of the patient. The models will modulate the power delivered by applicator(s) to deliver a conformal lethal dose. Problems inherent to computer driven MRgLITT have been posed as PDE constrained optimization problems; within the perspective of a clinical setting, the overhead associated with the solution to these inverse problems requires at least an order of magnitude speedup to allow treatment protocol design that is able to calibrate and recompute optimal parameters instantaneously. Alternative frameworks are being explored, such as state space control theory, to

achieve the required performance. The likely solution will be a coalescence of multiple frameworks.

Finally, the mathematical modeling and optimization of the treatment must be extended beyond traditional computational capabilities of single deterministic prediction to realistic stochastic systems. Stochastic computational approaches embody useful statistical information within expected values and standard deviations of predicted treatment outcomes that are clinically familiar to physicians. Computational methodologies must be developed under an uncertainty quantification framework [24, 14] that anticipates and accounts for potential complications concerning a given treatment. Uncertainty that may arise in the model prediction from any combination of possible inaccuracies in the probe placement, unaligned registration, or inaccurate patient model parameters will be propagated in the model prediction to statistically characterize the treatment. Under the stochastic framework, the MR-gLITT computational tools will provide a degree of confidence in the computational predictions directly proportional to the quality of the patient specific model parameters known at LITT time.

DDAS methodologies combined with minimally invasive approaches to surgery have significant potential to dramatically improve cancer therapies and enhance the quality of life of cancer patients. A few of the many factors and complexities that must be overcome to advance this particular DDAS implementation within a clinical setting has been presented. Current work focuses on LITT and MRTI as the thermal and imaging modalities, but the technology developed is adaptable to other MR-guided thermal therapies, such as focused ultrasound. Computationally, changing the thermal source or imaging modality amounts to utilizing a different source term in the governing PDE or adjoint problem, respectively. We are optimistic that these methodologies of computer modeling and simulation interacting with medical technologies have the potential to be extended to many target tissues and significantly enhance many areas of thermal therapy, including RF, microwave, ultrasound, and even cryotherapy applicators.

Acknowledgements The research in this chapter was supported in part through 5T32CA119930-03 and K25CA116291 NIH funding mechanisms and the National Science Foundation under grant CNS-0540033. The authors acknowledge the important support of DDAS research by Dr. Frederica Darema of NSF. During the course of this work we benefited from advice and comments of many colleagues, we mention in particular, C. Bajaj, J. C. Browne, I. Babuška, J. Bass, L. Bidaut, L. Demkowicz, S. Goswami, A. Hawkins, S. Khoshnevis, B. Kwon, and S. Prudhomme. The authors would like to thank Drs. Ashok Gowda and Roger McNichols from BioTex Inc. for providing the Visualase® System and altering the software so that it may be remotely controlled. The authors would also like to thank the ITK [16], Paraview [15], PETSc [2], TAO [3], libMesh [17], and CUBIT [23] communities for providing truly enabling software for real-time scientific computation and visualization.

References

1. D. E. Atkins, K. K. Droegemeier, S. I. Feldman, H. Garcia-Molina, M. L. Klein, D. G. Messerschmitt, P. Messina, J. P. Ostriker, and M. H. Wright. Revolutionizing science and engineering through cyberinfrastructure: Report of the national science foundation blue-ribbon advisory panel on cyberinfrastructure. Technical report, National Science Foundation, 2003.
2. Satish Balay, William D. Gropp, Lois C. McInnes, and Barry F. Smith. Petsc users manual. Technical Report ANL-95/11 - Revision 2.1.5, Argonne National Laboratory, 2003.
3. Steven J. Benson, Lois Curfman McInnes, Jorge Moré, and Jason Sarich. TAO user manual (revision 1.8). Technical Report ANL/MCS-TM-242, Mathematics and Computer Science Division, Argonne National Laboratory, 2005. <http://www.mcs.anl.gov/tao>.
4. A. Carpentier, RJ McNichols, RJ Stafford, J. Itzcovitz, JP Guichard, D. Reizine, S. Delaloge, E. Vicaut, D. Payen, A. Gowda, et al. Real-time magnetic resonance-guided laser thermal therapy for focal metastatic brain tumors. *Neurosurgery*, 63(1 Suppl 1):8, 2008.
5. C.K. Charny. Mathematical models of bioheat transfer. *Adv. Heat Trans.*, 22:19–155, 1992.
6. K. R. Diller, J. T. Oden, C. Bajaj, J. C. Browne, J. Hazle, I. Babuška, J. Bass, L. Bidaut, L. Demkowicz, A. Elliott, Y. Feng, D. Fuentes, S. Goswami, A. Hawkins, S. Khoshnevis, B. Kwon, S. Prudhomme, and R. J. Stafford. *Advances in Numerical Heat Transfer*, volume 3: Numerical Implementation of Bioheat Models and Equations, chapter 9: Computational Infrastructure for the Real-Time Patient-Specific Treatment of Cancer. Taylor & Francis Group, 2008.
7. A.M. Elliott, J. Schwartz, J. Wang, A.M. Shetty, C. Bourgoynne, D.P. O'Neal, J.D. Hazle, and R.J. Stafford. Quantitative comparison of delta P1 versus optical diffusion approximations for modeling near-infrared gold nanoshell heating. *Medical Physics*, 36:1351, 2009.
8. Y. Feng, D. Fuentes, A. Hawkins, J. Bass, M. N. Rylander, A. Elliott, A. Shetty, R. J. Stafford, and J. T. Oden. Nanoshell-mediated laser surgery simulation for prostate cancer treatment. *Engineering with Computers*, 25(1):3–13, 2009.
9. Y. Feng, J. T. Oden, and M.N. Rylander. A statistical thermodynamics based cell damage models and its validation in vitro. *J. Biomech. Eng.*, 130(041016):1–10, 2008.
10. Y. Feng, M. N. Rylander, J. Bass, J. T. Oden, and K. Diller. Optimal design of laser surgery for cancer treatment through nanoparticle-mediated hyperthermia therapy. In *NSTI-Nanotech 2005*, volume 1, pages 39–42, 2005.
11. D. Fuentes. *Computational Modeling and Real-Time Control of Patient-Specific Laser Treatment of Prostate Cancer*. PhD thesis, The University of Texas at Austin, 2008.
12. D. Fuentes, Y. Feng, A. Elliott, A. Shetty, R. J. McNichols, J. T. Oden, and R. J. Stafford. Adaptive Real-Time Bioheat Transfer Models for Computer Driven MR-guided Laser Induced Thermal Therapy. *IEEE Trans. BME*, 2009. submitted for publication.
13. D. Fuentes, J. T. Oden, K. R. Diller, J. Hazle, A. Elliott, A. Shetty, and R. J. Stafford. Computational modeling and real-time control of patient-specific laser treatment cancer. *Ann. BME.*, 37(4):763, 2009. DOI 10.1007/s10439-008-9631-8.
14. M.S. Grewal and A.P. Andrews. *Kalman filtering: theory and practice using MATLAB*. Wiley New York, 2001.
15. A. Henderson and J. Ahrens. *The ParaView Guide*. Kitware, 2004.
16. L. Ibanez, W. Schroeder, L. Ng, and J. Cates. *The ITK Software Guide*. Kitware, Inc. ISBN 1-930934-15-7, <http://www.itk.org/ItkSoftwareGuide.pdf>, second edition, 2005.
17. B.S. Kirk and JW Peterson. libMesh-a C++ Finite Element Library. *CFDLab*. URL <http://libmesh.sourceforge.net>, 2003.
18. J. Liu, L. Zhu, and L. Xu. Studies on the three-dimensional temperature transients in the canine prostate during transurethral microwave thermal therapy. *J. Biomech. Engr*, 122:372–378, 2000.
19. J. T. Oden, K. R. Diller, C. Bajaj, J. C. Browne, J. Hazle, I. Babuška, J. Bass, L. Demkowicz, Y. Feng, D. Fuentes, S. Prudhomme, M. N. Rylander, R. J. Stafford, and Y. Zhang. Dynamic data-driven finite element models for laser treatment of prostate cancer. *Num. Meth. PDE.*, 23(4):904–922, 2007.

20. H. H. Pennes. Analysis of tissue and arterial blood temperatures in the resting forearm. *J. Appl. Physiol.*, 1:93–122, 1948.
21. SA Prahl, M. Keijzer, SL Jacques, and AJ Welch. A Monte Carlo model of light propagation in tissue. *Dosimetry of Laser Radiation in Medicine and Biology*, 155:102–111.
22. M.N. Rylander. *Design of Hyperthermia Protocols for Inducing Cardiac Protection and Tumor Destruction by Controlling Heat Shock Protein Expression*. PhD thesis, The University of Texas at Austin, 2005.
23. T. Blacker *et al.* Cubit Users Manual, 2008. <http://cubit.sandia.gov/documentation>.
24. A. Tarantola. *Inverse Problem Theory and Methods for Model Parameter Estimation*. Society for Industrial and Applied Mathematics, 2005.
25. A. Wambersie and T. Landberg. ICRU Report 62: Prescribing, Recording and Reporting Photon Beam Therapy (Supplement to ICRU Report 50). *Bethesda, MD: International Commission on Radiation Units and Measurements*, 1999.
26. A. J. Welch and M. J. C. van Gemert. *Optical-Thermal Response of Laser-Irradiated Tissue*. New York: Plenum Press, 1995.
27. E. H. Wissler. Pennes' 1948 paper revisited. *J. Appl. Physiol.*, 85:35–41, 1998.